Boundary Value Problems
a SpringerOpen Journal

RESEARCH   **Open Access**

Dual solutions of stagnation-point flow of a nanofluid over a stretching surface

Peri K Kameswaran[1], Precious Sibanda[1*], Chetteti RamReddy[2] and Prabhala VSN Murthy[3]

*Correspondence:
sibandap@ukzn.ac.za
[1] School of Mathematical Sciences,
University of KwaZulu-Natal, Private
Bag X01, Scottsville,
Pietermaritzburg, 3209, South Africa
Full list of author information is
available at the end of the article

Abstract

The paper discusses the effects of homogeneous-heterogeneous reactions on stagnation-point flow of a nanofluid over a stretching or shrinking sheet. The model presented describes mass transfer in copper-water and silver-water nanofluids. The governing system of equations is solved numerically, and the study shows that dual solutions exist for certain suction/injection, stretching/shrinking and magnetic parameter values. Comparison of the numerical results is made with previously published results for special cases.

Keywords: homogeneous-heterogeneous reactions; nanofluids; volume fraction model; stretching or shrinking sheet; magnetic field strength

1 Introduction

Problems involving fluid flow over stretching or shrinking surfaces can be found in many manufacturing processes such as in polymer extrusion, wire and fiber coating, foodstuff processing, *etc.* Crane [1] was the first to consider the steady two-dimensional flow of a Newtonian fluid driven by a stretching elastic flat sheet which moved in its own plane with velocity varying linearly with the distance from a fixed point. This study was subsequently extended by many authors to explore various aspects of heat transfer in a fluid surrounding a stretching sheet (Tsou *et al.* [2], Erickson *et al.* [3], Mucoglu and Chen [4], Grubka and Bobba [5], Karwe and Jaluria [6], Chen [7], Abo-Eldahab and El-Aziz [8], Salem and El-Aziz [9], Ali [10], Ishak *et al.* [11]).

The magnetohydrodynamic effect has important engineering applications in electrical motors. Heat transfer over a stretching or shrinking sheet subject to an external magnetic field, viscous dissipation and joule effects was studied by Jafar *et al.* [12]. They observed that the flow and heat transfer characteristics for a shrinking sheet were quite different from those of a stretching sheet. Lok *et al.* [13] analyzed MHD stagnation-point flow from a shrinking sheet. They found that dual solutions existed for small values of the magnetic parameter. The stagnation-point flow over a stretching or shrinking sheet in a nanofluid was investigated by Bachok *et al.* [14]. They showed that adding nanoparticles to a base fluid increased the skin friction and heat transfer coefficients. Recently, Narayana and Sibanda [15] investigated the laminar flow of a nanoliquid film over an unsteady stretching sheet. They noticed that the effect of an increase in the nanoparticle volume fraction was to reduce the axial velocity and free stream velocity in the case of a Cu-water nanoliquid. However, the opposite appeared to be true in the case of an Al_2O_3-water nanofluid. Kameswaran *et al.* [16] studied the effects of viscous dissipation and a chemical reaction in

hydromagnetic nanofluid flow due to a stretching or shrinking sheet. They found that the velocity profiles decreased with an increase in the nanoparticle volume fraction, while the opposite was true in the case of temperature and concentration profiles. The study further showed that liquids with nanoparticle suspensions were better suited for effective cooling of the stretching sheet due to their enhanced conductivity and thermal properties.

Most chemically reacting systems involve both homogeneous and heterogeneous reactions (combustion, catalysis and biochemical systems). The simple combustion model helps us to understand the combustion phenomenon in many complex engineering applications such as in aircraft and rocket engines. A model for isothermal homogeneous-heterogeneous reactions in the boundary layer flow of a viscous fluid past a flat plate was presented by Merkin [17]. He modeled the homogeneous reaction by a cubic autocatalysis process and the heterogeneous reaction by a first-order process. Chaudhary and Merkin [18] analyzed homogeneous-heterogeneous reactions in boundary layer flow. They presented a numerical solution of the boundary layer equations near the leading edge of a flat plate. Ziabakhsh *et al.* [19] studied the diffusion of a chemically reactive species into a nonlinearly stretching sheet immersed in a porous medium. Chambre and Acrivos [20] studied isothermal chemical reactions on laminar boundary layer flow. The two-dimensional stagnation-point flow near an infinite permeable wall with a homogeneous-heterogeneous reaction was studied by Khan and Pop [21], while Khan and Pop [22] and Bachok *et al.* [23] studied the effects of homogeneous-heterogeneous reactions on fluid flow due to a stretching sheet. Recently, the effects of homogeneous-heterogeneous reactions in nanofluid flow due to a porous stretching sheet were studied by Kameswaran *et al.* [24]. They found that the concentration at the surface decreased with the strength of the heterogeneous reaction. In the case of a shrinking sheet, they showed that the velocity profiles decreased with increasing nanoparticle volume fraction in the case of a Cu-water nanofluid.

This article presents a study of homogeneous-heterogeneous reactions on MHD nanofluid stagnation point flow due to a stretching or shrinking sheet. The transformed nonlinear conservation equations are solved numerically.

2 Mathematical formulation

Consider a two-dimensional steady boundary layer flow of an incompressible nanofluid over a stretching or shrinking sheet. A Cartesian co-ordinate system is used with the x-axis along the sheet and the y-axis normal to the sheet. The flow configuration and the coordinate system are shown in Figure 1. The velocity of the outer flow is of the form $u_e(x) = U_\infty x$ and the velocity of the stretching or shrinking sheet is $u_w(x) = U_w x$, where U_w and U_∞

Figure 1 Physical model and coordinate system.
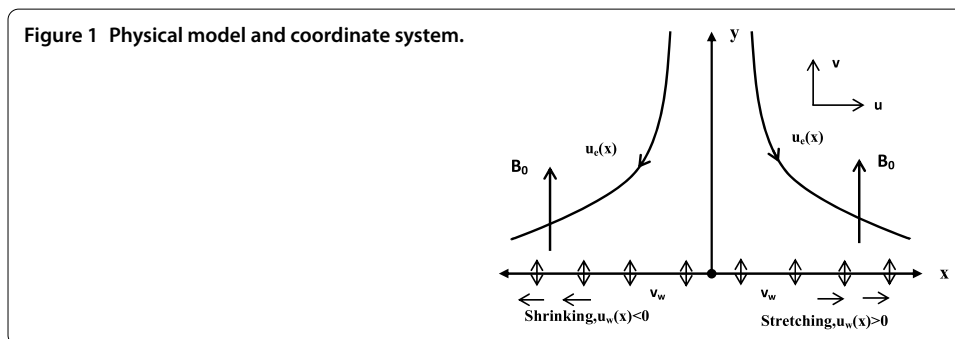
are constants. The fluid is a water-based nanofluid containing copper (Cu) or silver (Ag) nanoparticles. The base fluid and the nanoparticles are in thermal equilibrium with no slip occurring between them. We assume the simple homogeneous-heterogeneous reaction model proposed by Chaudhary and Merkin [18] of the form

$$A + 2B \rightarrow 3B, \qquad \text{rate} = k_c ab^2, \tag{1}$$
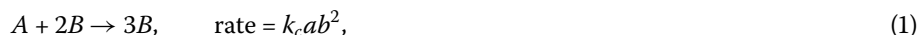
while on the catalyst surface we have the single, isothermal, first-order reaction

$$A \rightarrow B, \qquad \text{rate} = k_s a, \tag{2}$$

where a and b are the concentrations of the chemical species A and B, and k_c and k_s are the rate constants. We assume that both reaction processes are isothermal. Under these assumptions, the boundary layer equations governing the flow can be written in the dimensional form [18, 25]

$$\frac{\partial u}{\partial x} + \frac{\partial v}{\partial y} = 0, \tag{3}$$

$$u\frac{\partial u}{\partial x} + v\frac{\partial u}{\partial y} = \frac{\mu_{nf}}{\rho_{nf}}\frac{\partial^2 u}{\partial y^2} + u_e(x)\frac{du_e(x)}{dx} + \frac{\sigma B_0^2}{\rho_{nf}}\big[u_e(x) - u\big], \tag{4}$$

$$u\frac{\partial a}{\partial x} + v\frac{\partial a}{\partial y} = D_A\frac{\partial^2 a}{\partial y^2} - k_c ab^2, \tag{5}$$

$$u\frac{\partial b}{\partial x} + v\frac{\partial b}{\partial y} = D_B\frac{\partial^2 b}{\partial y^2} + k_c ab^2. \tag{6}$$

The boundary conditions for equations (3)-(6) are given in the form

$$u = u_w(x), \qquad v = v_w, \qquad D_A\frac{\partial a}{\partial y} = k_s a, \qquad D_B\frac{\partial b}{\partial y} = -k_s a \quad \text{at } y = 0,$$

$$u = u_e(x), \qquad a \rightarrow a_0, \qquad b \rightarrow 0 \quad \text{as } y \rightarrow \infty, \tag{7}$$

where u, v are the velocity components in the x and y directions, respectively, D_A and D_B are the respective diffusion species coefficients of A and B, a_0 is a positive constant. The effective dynamic viscosity of the nanofluid was given by Brinkman [26] as

$$\mu_{nf} = \frac{\mu_f}{(1 - \phi)^{2.5}}, \tag{8}$$

where ϕ is the solid volume fraction of nanoparticles. The effective density of the nanofluids is given as

$$\rho_{nf} = (1 - \phi)\rho_f + \phi\rho_s. \tag{9}$$

Here, the subscripts nf, f and s represent the thermophysical properties of the nanofluid, the base fluid and nanoparticles, respectively.

The continuity equation (3) is satisfied by introducing a stream function ψ such that

$$u = \frac{\partial \psi}{\partial y} \quad \text{and} \quad v = -\frac{\partial \psi}{\partial x},$$ (10)

where $\psi = (U_\infty \nu_f)^{\frac{1}{2}} x f(\eta)$, $f(\eta)$ is the dimensionless stream function and $\eta = (U_\infty / \nu_f)^{\frac{1}{2}} y$.

The velocity components are given by

$$u = U_\infty x f'(\eta) \quad \text{and} \quad v = -(U_\infty \nu_f)^{\frac{1}{2}} f(\eta).$$ (11)

The concentrations of the chemical species A and B are represented as

$$a = a_0 g(\eta) \quad \text{and} \quad b = a_0 h(\eta),$$ (12)

where $g(\eta)$ and $h(\eta)$ are dimensionless concentrations. On using equations (8), (9), (11) and (12), equations (4)-(7) transform to the following two-point boundary value problem:

$$f''' + \phi_1 \left[ff'' - f'^2 + 1 + \frac{M}{\phi_2}(1 - f') \right] = 0,$$ (13)

$$\frac{1}{Sc} g'' + fg' - Kgh^2 = 0,$$ (14)

$$\frac{\delta}{Sc} h'' + fh' + Kgh^2 = 0,$$ (15)

$$f(0) = f_w, \qquad f'(0) = \lambda, \qquad f'(\eta) \to 1 \quad \text{as } \eta \to \infty,$$ (16)

$$g'(0) = K_s g(0), \qquad g(\eta) \to 1 \quad \text{as } \eta \to \infty,$$ (17)

$$\delta h'(0) = -K_s g(0), \qquad h(\eta) \to 0 \quad \text{as } \eta \to \infty.$$ (18)

The non-dimensional parameters in equations (13)-(18) are the magnetic parameter M, the Schmidt number Sc, the measure of the strength of the homogeneous reaction K, the ratio of diffusion coefficients δ, the mass transfer parameter f_w, with $f_w > 0$ for suction and $f_w < 0$ for injection, the measure of the strength of the heterogeneous reaction K_s, the Reynolds number Re and $\lambda = U_w / U_\infty$ is the stretching parameter, with $\lambda > 0$ for stretching and $\lambda < 0$ for shrinking, respectively. These parameters are respectively defined as

$$M = \frac{\sigma B_0^2}{\rho_f U_\infty}, \qquad Sc = \frac{\nu_f}{D_A}, \qquad K = \frac{k_c a_0^2}{U_\infty}, \qquad \delta = \frac{D_B}{D_A},$$ (19)

$$f_w = -\frac{v_w}{\sqrt{U_\infty \nu_f}}, \qquad K_s = \frac{k_s l}{D_A} Re^{-\frac{1}{2}}, \qquad Re = \frac{U_\infty l}{\nu_f},$$ (20)

where

$$\left. \begin{array}{l} \phi_1 = (1 - \phi)^{2.5} [1 - \phi + \phi(\frac{\rho_s}{\rho_f})], \\ \phi_2 = 1 - \phi + \phi(\frac{\rho_s}{\rho_f}). \end{array} \right\}$$ (21)

In most applications, we expect the diffusion coefficients of chemical species A and B to be of a comparable size. This leads us to making a further assumption that the diffusion

coefficients D_A and D_B are equal, *i.e.*, $\delta = 1$ (Chaudhary and Merkin [18]). In this case we have, from equations (16), (17) and (18),

$$g(\eta) + h(\eta) = 1. \tag{22}$$

Thus equations (14) and (15) reduce to

$$\frac{1}{Sc}g'' + fg' - Kg(1-g)^2 = 0, \tag{23}$$

subject to the boundary conditions

$$g'(0) = K_s g(0), \qquad g(\eta) \to 1 \quad \text{as } \eta \to \infty. \tag{24}$$

It is quite straightforward to show that the skin friction coefficient C_f, which characterizes the surface drag, is given by

$$C_f (1-\phi)^{2.5} \sqrt{Re_x} = -2f''(0), \tag{25}$$

where $Re_x = xu_e(x)/\nu_f$ is the local Reynolds number.

3 Results and discussion

The system of ordinary differential equations (13) and (23) with boundary conditions (16) and (24) was solved numerically using Matlab `bvp4c` routine. We considered Cu-water and Ag-water nanofluids. The thermophysical properties of the nanofluids used in this paper are given in Table 1.

In order to determine the accuracy of our numerical results, the present results for the skin-friction coefficient $f''(0)$ were compared with the available published results of Jafar *et al.* [12], Bachok *et al.* [23] and Wang [28] in Tables 2, 3 and 4.

Tables 2 and 3 give the coefficient $f''(0)$ for different parameter values. Table 2 gives a comparison of the present results with those obtained by Jafar *et al.* [12] and Wang [28] when $M = K = K_s = Sc = f_w = \phi = 0$, for different values of the stretching parameter. We observe that for increasing λ, the present results are in good agreement with results in the literature.

Table 1 Thermophysical properties of water, Cu-water and Ag-water nanofluids, Oztop and Abu-Nada [27]

Properties →	ρ (kg/m³)	C_p (J/kgK)	k (W/mK)
Pure water	997.1	4,179	0.613
Cu	8,933	385	401
Ag	10,500	235	429

Table 2 Comparison of $f''(0)$ from current results with Wang [28] and Jafar *et al.* [12] for various values of λ for the stretching sheet when $M = Sc = f_w = K_s = 0$ and $\phi = 0$

λ	0	0.1	0.2	0.5	1	2	5
Wang [28]	1.232588	1.14656	1.05113	0.71330	0	−1.88731	−10.26475
Jafar *et al.* [12]	1.2326	1.1466	1.0511	0.7133	0	−1.8873	−10.2648
Present	1.232588	1.146561	1.051130	0.713295	0	−1.887307	−10.264749

Table 3 Comparison of $f''(0)$ from current results with Wang [28] and Jafar *et al.* [12] for various values of λ for the shrinking sheet when $M = K = Sc = f_w = K_s = 0$ and $\phi = 0$

λ	−0.25	−0.5	−0.75	−1	−1.2465
Wang [28]	1.40224	1.49576	1.48930	1.32882	0.55430
Jafar *et al.* [12]	1.4022	1.4957	1.4893	1.3288	0.5543
Present	1.402241	1.495670	1.489298	1.328817	0.554296

Table 4 Comparison of $f''(0)$ obtained by Bachok *et al.* [23] with the present results for particular values of $K_s = K = Sc = 1$, $f_w = M = \phi = 0$

λ	$f_1''(0)$ [23]	$f_1''(0)$ (Present)	$f_2''(0)$ [23]	$f_2''(0)$ (Present)
−1.15	1.0822	1.08223	0.1167	0.11670
−1.20	0.9325	0.93247	0.2336	0.23365
−1.21	0.8921	0.89209	0.2679	0.26789
−1.22	0.8451	0.84511	0.3088	0.30885
−1.23	0.7874	0.78744	0.3606	0.36062
−1.24	0.7066	0.70661	0.4357	0.43567
−1.242	0.6838	0.68376	0.4574	0.45738
−1.244	0.6551	0.65508	0.4849	0.48492
−1.246	0.6098	0.60983	0.5290	0.52903

Figure 2 Effects of λ on velocity, when $K = 1$, $Sc = 1$, $K_s = 1$, $M = 0.5$, $f_w = 1$.
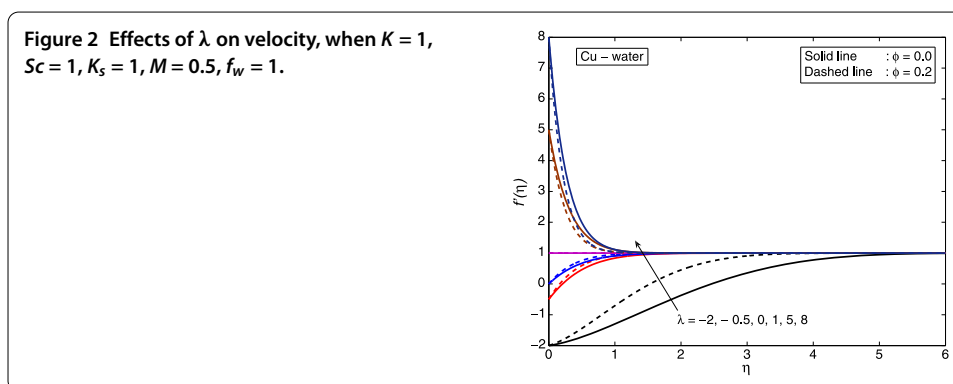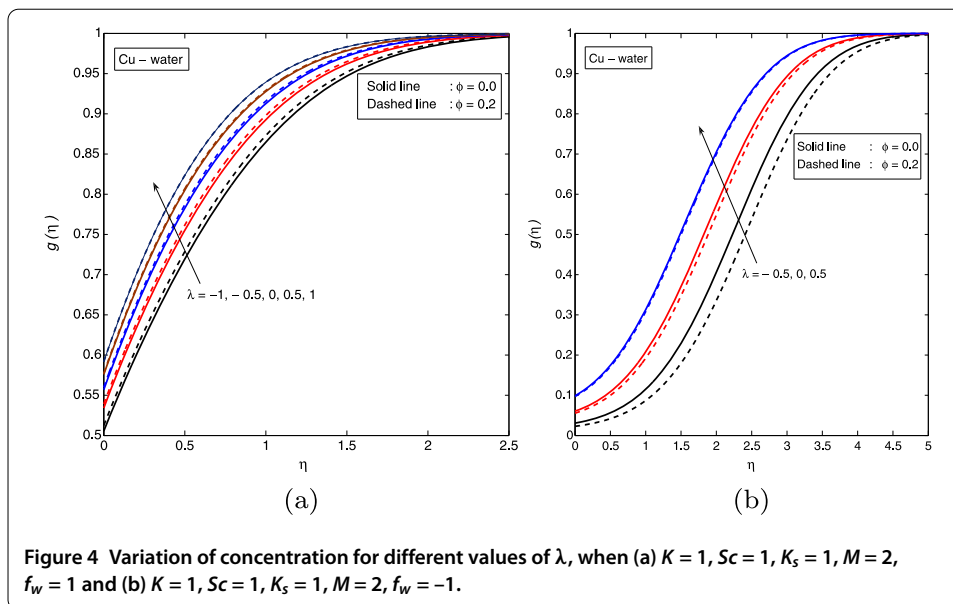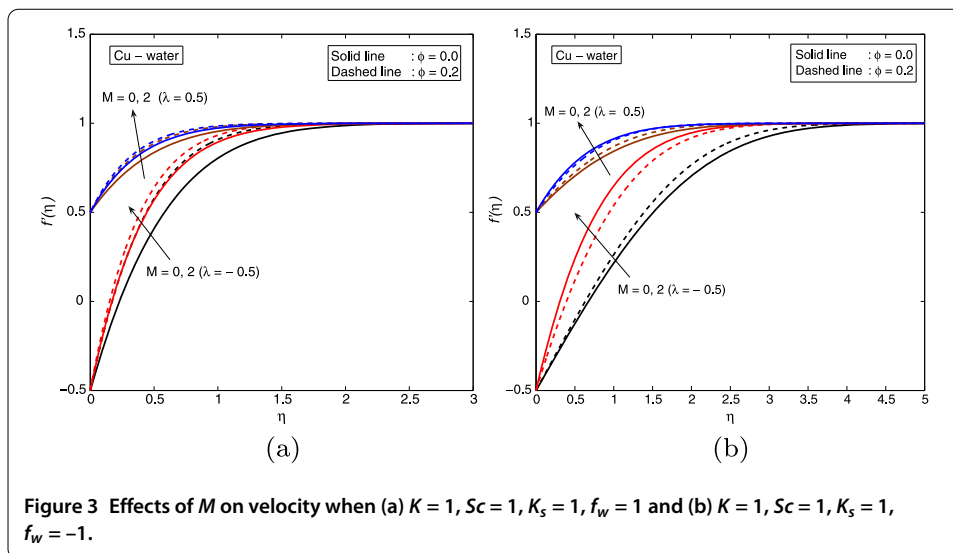
Table 4 gives the values of $f''(0)$ for selected λ when $K_s = K = Sc = 1$, $f_w = M = \phi = 0$. We note here that with decreasing λ the first solution $f_1''(0)$ decreases while the second solution $f_2''(0)$ increases. These results are in good agreement with the results obtained by Bachok *et al.* [23] in the absence of the particular physical parameter.

The effects of the Schmidt number, stretching, magnetic and chemical reaction parameters are shown in Figures 2-12.

Figure 2 shows the effects of both stretching and shrinking on the velocity profiles in the case of a Cu-water nanofluid. We observe that in both cases, the velocity profiles increase with the parameter λ. Further, we note that for a shrinking sheet, the velocity in the case of a Cu-water nanofluid is larger than that of a clear fluid. The opposite is, however, true for the case of a stretching sheet. The momentum boundary layer thickness decreases as λ increases and the flow has an inverted boundary layer structure when $\lambda < 1$. The findings in the case of a clear fluid are similar to the results obtained by Jat and Chaudhary [29].
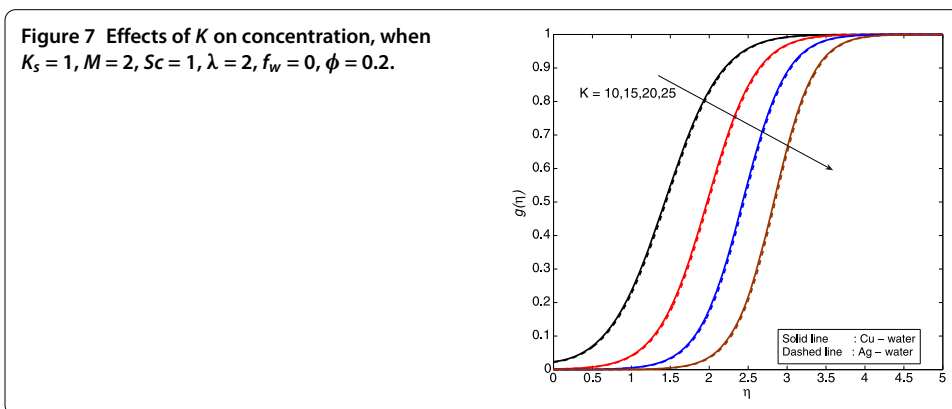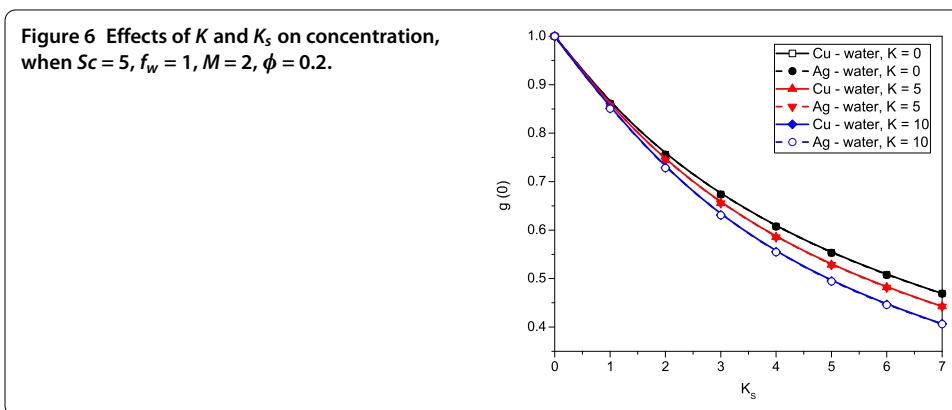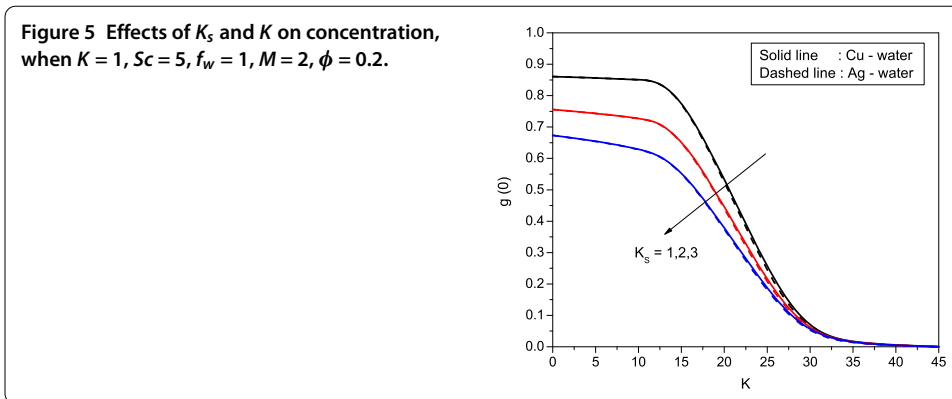
Figures 3(a) and 3(b) illustrate the effect of the magnetic parameter, nanoparticle volume fraction and stretching or shrinking parameters on the velocity profiles. We note that for both stretching and shrinking sheets, the fluid velocity increases with λ and M. Furthermore, increasing the value of M also causes thinning of the boundary layer. This implies

Figure 3 Effects of *M* on velocity when (a) *K* = 1, *Sc* = 1, *K_s* = 1, *f_w* = 1 and (b) *K* = 1, *Sc* = 1, *K_s* = 1, *f_w* = −1.

Figure 4 Variation of concentration for different values of λ, when (a) *K* = 1, *Sc* = 1, *K_s* = 1, *M* = 2, *f_w* = 1 and (b) *K* = 1, *Sc* = 1, *K_s* = 1, *M* = 2, *f_w* = −1.

an increase in the velocity gradient $f''(0)$. Thus the magnetic field enhances the fluid motion in the boundary layer in the case of a clear fluid. The same trend is observed in the case of a Cu-water nanofluid. We also observe in the case of injection that, with increasing magnetic parameter, the increment in the momentum boundary layer is more significant than in the case of suction.

Figures 4(a) and 4(b) illustrate the effects of the stretching or shrinking parameter and volume fraction on the solute concentration when $K = 1$, $Sc = 1$, $K_s = 1$, $M = 2$, $f_w = 1$. We observe that the concentration profiles increase with the stretching parameter. We note also that the concentration increases as λ varies from λ = −1 to λ = 1 for both the clear fluid and the Cu-water nanofluid. However, beyond λ = 1, the opposite is true for the clear fluid and the Cu-water nanofluid.

The variation of $g(0)$ for different values of K and K_s is shown in Figures 5 and 6, respectively. From Figure 5 we observe that the concentration at the surface decreases as the

Figure 5 Effects of K_s and K on concentration, when $K = 1$, $Sc = 5$, $f_w = 1$, $M = 2$, $\phi = 0.2$.

Figure 6 Effects of K and K_s on concentration, when $Sc = 5$, $f_w = 1$, $M = 2$, $\phi = 0.2$.

Figure 7 Effects of K on concentration, when $K_s = 1$, $M = 2$, $Sc = 1$, $\lambda = 2$, $f_w = 0$, $\phi = 0.2$.

strength of the heterogeneous reaction increases. This is simply explained by the fact that the strength of the chemical reaction depends on the concentration. On the other hand, from Figure 6, we found that $g(0)$ decreases with increasing K and K_s. These findings are similar to the results reported by Kameswaran *et al.* [24].

Figures 7 and 8 show the effects of K and λ on the concentration when the other parameters are fixed. We note, as expected, that the wall concentration decreases as the strength of the homogeneous reaction increases. The level of decrease is, however, more significant in the case of Ag-water than for Cu-water. Figure 8 shows the influence of stretching on the concentration profiles. It can be seen that the concentration decreases when the sheet is shrunk and increases with stretching.

Figure 8 Effects of λ on concentration, when M = 2, Sc = 1, f_w = 0, K = 20, K_s = 0.5.
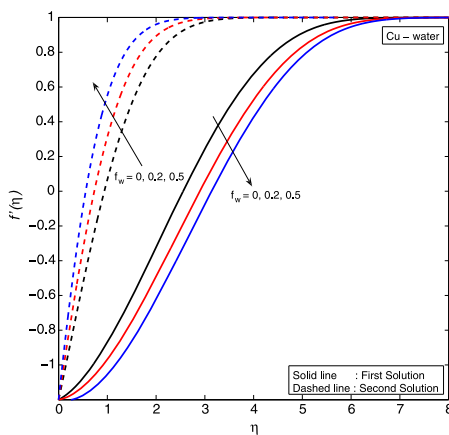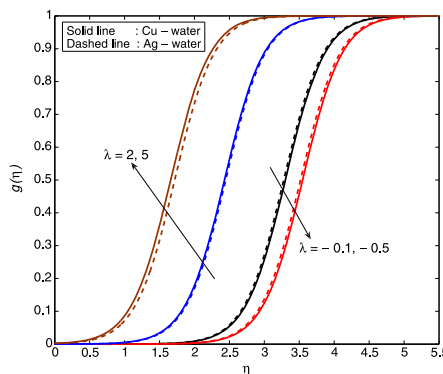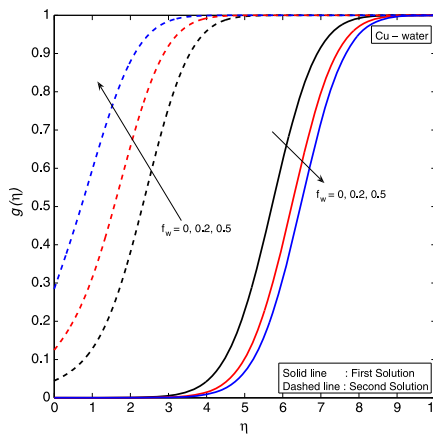
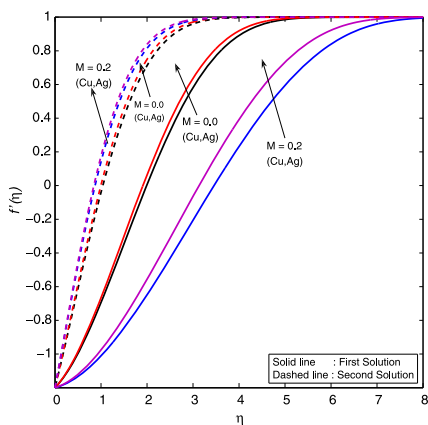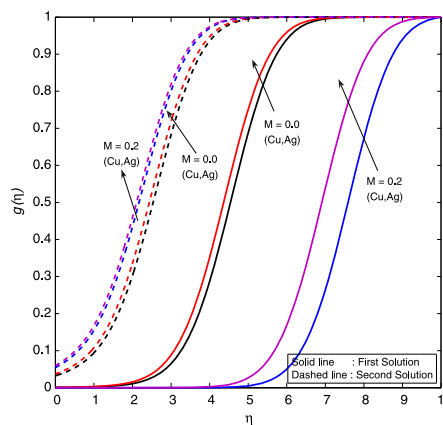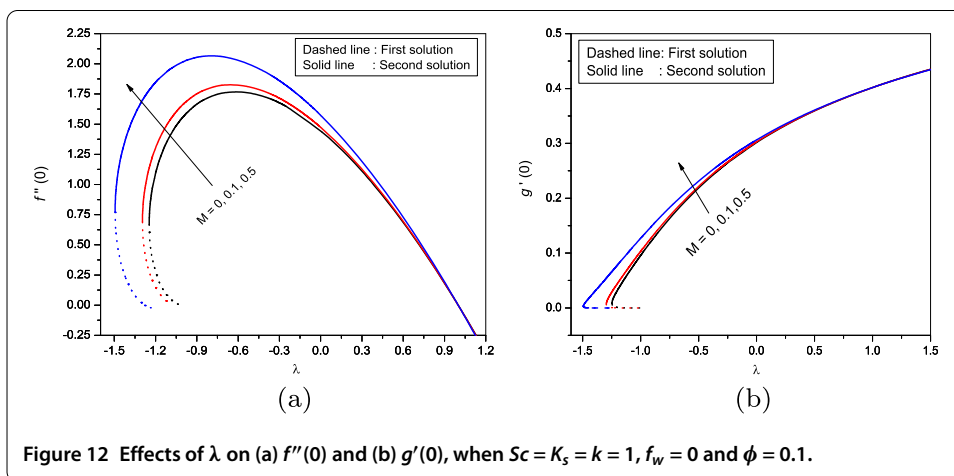**Figure 9 Effects of f_w on (a) velocity and (b) concentration profiles, when M = 0.1, Sc = 1, K_s = 1, K = 1, φ = 0.1 and λ = −1.2.**
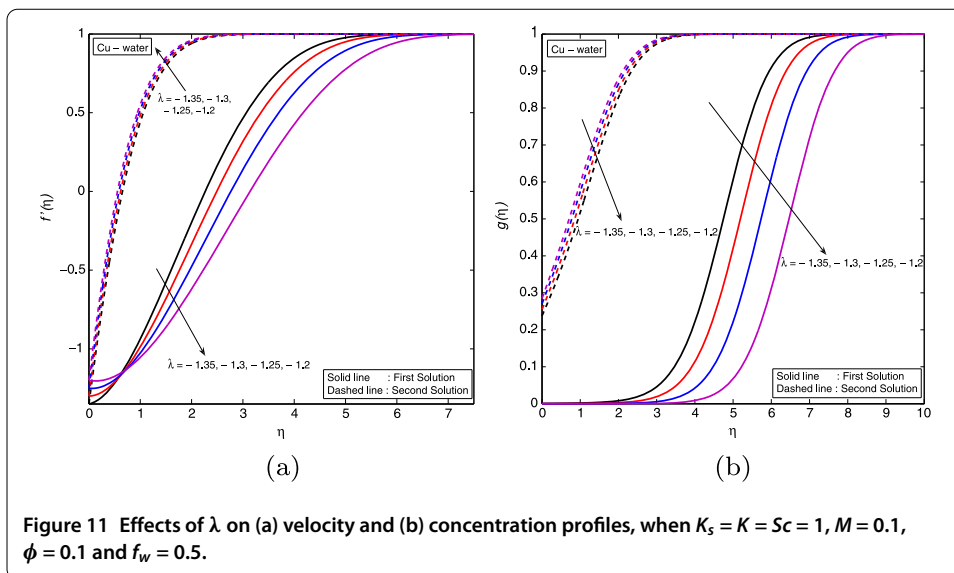

Figure 10 Effects of magnetic parameter M on (a) velocity and (b) concentration profiles, when K_s = 1, K = 1, Sc = 1, f_w = 0, φ = 0.1 and λ = −1.2.

Figure 11 Effects of λ on (a) velocity and (b) concentration profiles, when $K_s = K = Sc = 1$, $M = 0.1$, $\phi = 0.1$ and $f_w = 0.5$.

Figure 12 Effects of λ on (a) $f''(0)$ and (b) $g'(0)$, when $Sc = K_s = k = 1$, $f_w = 0$ and $\phi = 0.1$.

The effects of suction/injection parameter f_w on the velocity and concentration profiles are presented in Figure 9 for a Cu-water nanofluid. These profiles are qualitatively similar to the profiles obtained in the case of a clear fluid. Here we note dual solutions, *i.e.*, the first and second solutions. The velocity and concentration profiles decrease with increasing $f_w > 0$ in the case of the first solution. The opposite is, however, true in the case of the second solution. The far field boundary conditions are asymptotically satisfied, thus supporting the validity of the numerical solutions and the existence of dual solutions. In Figure 9(b), the concentration increases more rapidly with increasing suction/injection in the case of the second solution.

Figure 10 shows the effect of the magnetic parameter on $f'(\eta)$ and $g(\eta)$ for both Ag-water and Cu-water nanofluids. The velocity and concentration profiles are higher for Cu particles compared to Ag nanoparticles in the absence of the magnetic parameter. Increasing the value of M causes thinning of the boundary layer. The magnetic field enhances the fluid motion at the boundary, and for clear fluids these results are similar to well-known results in the literature.

The variation of the velocity and concentration profiles with the stretching/shrinking parameter is shown in Figure 11. The dual velocity $f'(\eta)$ and concentration $g(\eta)$ profiles decrease with an increase in the magnitude of λ in the case of the first solution and increases in the case of the second solution. It is to be noted that momentum boundary layer thickness for the second solution is thicker than for the first solution. For the case of a clear fluid, the results are similar to those obtained by Bhattacharyya [30]. We also note that the velocity gradient at the surface increases with λ, which is consistent with the results predicted from the computation of the skin friction coefficient.

The variation of the reduced skin friction coefficient $f''(0)$ with λ is shown in Figure 12(a). The values of $f''(0)$ are positive when $\lambda < 1$ and negative when $\lambda > 1$. Physically, a positive $f''(0)$ implies that the fluid exerts a drag force on the plate and a negative sign implies the opposite. It is evident that dual solutions of equations (13) and (23) subject to the boundary conditions (16) and (24) exist when $\lambda < 0$. There is a critical value of $\lambda_c < 0$ for which the first and second solutions meet. This critical value depends on the values of the other embedded parameters, and we found, for instance, that $\lambda_c = -1.2465798095$ when $M = 0$, $\lambda_c = -1.295662771$ when $M = 0.1$ and $\lambda_c = -1.49444085032$ when $M = 0.5$. These results show that $|\lambda_c|$ increases with M. However, for $\lambda_c < \lambda \leq -1$, the solution is not unique, there being two solutions for each λ. Figure 12(b) shows that $g'(0)$ increases with the magnetic parameter M.

4 Conclusions

The effects of homogeneous-heterogeneous reactions in MHD nanofluid flow due to a stretching or shrinking sheet have been studied. The transformed governing nonlinear differential equations have been solved numerically. Dual solutions for the velocity and concentration distributions have been obtained for some values of the stretching/shrinking, suction/injection and magnetic parameters. The effects of physical and fluid parameters on the velocity, concentration and skin friction have been analyzed. It was observed that for both the cases of shrinking and stretching sheets, the fluid velocity increased with the magnetic parameter. The concentration at the surface decreased as the strength of heterogeneous reactions increased for both Cu-water and Ag-water nanofluids. The boundary layer thickness for the first solution is always thinner than that for the second solution.

Author details
[1]School of Mathematical Sciences, University of KwaZulu-Natal, Private Bag X01, Scottsville, Pietermaritzburg, 3209, South Africa. [2]Department of Mathematics, National Institute of Technology, Rourkela, Odisha 769008, India. [3]Department of Mathematics, Indian Institute of Technology, Kharagpur, 721302, India.

References
1. Crane, LJ: Flow past a stretching plate. Z. Angew. Math. Phys. **21**, 645-647 (1970)
2. Tsou, FK, Sparrow, EM, Goldstein, RJ: Flow and heat transfer in the boundary layer on a continuous moving surface. Int. J. Heat Mass Transf. **10**, 219-235 (1967)
3. Erickson, LE, Fan, LT, Fox, VG: Heat and mass transfer on a moving continuous flat plate with suction or injection. Ind. Eng. Chem. Fundam. **5**, 19-25 (1966)

4. Mucoglu, A, Chen, TS: Mixed convection on inclined surfaces. J. Heat Transf. **101**, 422-426 (1979)
5. Grubka, LJ, Bobba, KM: Heat transfer characteristics of a continuous, stretching surface with variable temperature. J. Heat Transf. **107**, 248-250 (1985)
6. Karwe, MV, Jaluria, Y: Fluid flow and mixed convection transport from a moving plate in rolling and extrusion processes. J. Heat Transf. **110**, 655-661 (1988)
7. Chen, CH: Laminar mixed convection adjacent to vertical, continuously stretching sheets. Heat Mass Transf. **33**, 471-476 (1998)
8. Abo-Eldahab, EM, El-Aziz, MA: Blowing/suction effect on hydromagnetic heat transfer by mixed convection from an inclined continuously stretching surface with internal heat generation/absorption. Int. J. Therm. Sci. **43**, 709-719 (2004)
9. Salem, AM, El-Aziz, MA: Effect of Hall currents and chemical reaction on hydromagnetic flow of a stretching vertical surface with internal heat generation/absorption. Appl. Math. Model. **32**, 1236-1254 (2008)
10. Ali, ME: Heat transfer characteristics of a continuous stretching surface. Wärme- Stoffübertrag. **29**, 227-234 (1994)
11. Ishak, A, Nazar, R, Pop, I: Boundary layer flow and heat transfer over an unsteady stretching vertical surface. Meccanica **44**, 369-375 (2009)
12. Jafar, K, Nazar, R, Ishak, A, Pop, I: MHD flow and heat transfer over stretching/shrinking sheets with external magnetic field, viscous dissipation and joule effects. Can. J. Chem. Eng. **90**, 1336-1346 (2012)
13. Lok, YY, Ishak, A, Pop, I: MHD stagnation-point flow towards a shrinking sheet. Int. J. Numer. Methods Heat Fluid Flow **21**, 61-72 (2011)
14. Bachok, N, Ishak, A, Pop, I: Stagnation point flow over a stretching/shrinking sheet in a nanofluid. Nanoscale Res. Lett. **6**, 623 (2011)
15. Narayana, M, Sibanda, P: Laminar flow of a nanoliquid film over an unsteady stretching sheet. Int. J. Heat Mass Transf. **55**, 7552-7560 (2012)
16. Kameswaran, PK, Narayana, M, Sibanda, P, Murthy, PVSN: Hydromagnetic nanofluid flow due to a stretching or shrinking sheet with viscous dissipation and chemical reaction effects. Int. J. Heat Mass Transf. **55**, 7587-7595 (2012)
17. Merkin, JH: A model for isothermal homogeneous-heterogeneous reactions in boundary layer flow. Math. Comput. Model. **24**, 125-136 (1996)
18. Chaudhary, MA, Merkin, JH: A simple isothermal model for homogeneous-heterogeneous reactions in boundary layer flow. I. Equal diffusivities. Fluid Dyn. Res. **16**, 311-333 (1995)
19. Ziabakhsh, Z, Domairry, G, Bararnia, H, Babazadeh, H: Analytical solution of flow and diffusion of chemically reactive species over a nonlinearly stretching sheet immersed in a porous medium. J. Taiwan Inst. Chem. Eng. **41**, 22-28 (2010)
20. Chambre, PL, Acrivos, A: On chemical surface reactions in laminar boundary layer flows. J. Appl. Phys. **27**, 1322-1328 (1956)
21. Khan, WA, Pop, I: Flow near the two-dimensional stagnation-point on an infinite permeable wall with a homogeneous-heterogeneous reaction. Commun. Nonlinear Sci. Numer. Simul. **15**, 3435-3443 (2010)
22. Khan, WA, Pop, I: Effects of homogeneous-heterogeneous reactions on the viscoelastic fluid toward a stretching sheet. J. Heat Transf. **134**, 064506 (2012)
23. Bachok, N, Ishak, A, Pop, I: On the stagnation-point flow towards a stretching sheet with homogeneous-heterogeneous reactions effects. Commun. Nonlinear Sci. Numer. Simul. **16**, 4296-4302 (2011)
24. Kameswaran, PK, Shaw, S, Sibanda, P, Murthy, PVSN: Homogeneous-heterogeneous reactions in a nanofluid flow due to a porous stretching sheet. Int. J. Heat Mass Transf. **57**, 465-472 (2013)
25. Tiwari, RK, Das, MK: Heat transfer augmentation in a two-sided lid-driven differentially heated square cavity utilizing nanofluids. Int. J. Heat Mass Transf. **50**, 2002-2018 (2007)
26. Brinkman, HC: The viscosity of concentrated suspensions and solutions. J. Chem. Phys. **20**, 571-581 (1952)
27. Oztop, HF, Abu-Nada, E: Numerical study of natural convection in partially heated rectangular enclosures filled with nanofluids. Int. J. Heat Fluid Flow **29**, 1326-1336 (2008)
28. Wang, CY: Stagnation flow towards a shrinking sheet. Int. J. Non-Linear Mech. **43**, 377-382 (2008)
29. Jat, RN, Chaudhary, S: MHD flow and heat transfer over a stretching sheet. Appl. Math. Sci. **3**, 1285-1294 (2009)
30. Bhattacharyya, K: Dual solutions in boundary layer stagnation-point flow and mass transfer with chemical reaction past a stretching/shrinking sheet. Int. Commun. Heat Mass Transf. **38**, 917-922 (2011)